VIP Smart Materials Very Important Paper

International Edition: DOI: 10.1002/anie.201611325
German Edition: DOI: 10.1002/ange.201611325

High-Power Actuation from Molecular Photoswitches in Enantiomerically Paired Soft Springs

Sarah J. Aßhoff, Federico Lancia, Supitchaya Iamsaard, Benjamin Matt, Tibor Kudernac, Stephen P. Fletcher, and Nathalie Katsonis**

Abstract: *Motion in plants often relies on dynamic helical systems as seen in coiling tendrils, spasmoneme springs, and the opening of chiral seedpods. Developing nanotechnology that would allow molecular-level phenomena to drive such movements in artificial systems remains a scientific challenge. Herein, we describe a soft device that uses nanoscale information to mimic seedpod opening. The system exploits a fundamental mechanism of stimuli-responsive deformation in plants, namely that inflexible elements with specific orientations are integrated into a stimuli-responsive matrix. The device is operated by isomerization of a light-responsive molecular switch that drives the twisting of strips of liquid-crystal elastomers. The strips twist in opposite directions and work against each other until the pod pops open from stress. This mechanism allows the photoisomerization of molecular switches to stimulate rapid shape changes at the macroscale and thus to maximize actuation power.*

Designing shape-morphing materials has become a major scientific challenge, with implications ranging from soft robotics[1–3] to realizing the full potential of artificial molecular machines.[4–8] The variety of movements seen in the plant and animal kingdoms have provided inspiration for the engineering of soft robots of all kinds,[9–14] and in particular, the realization that plant mechanics often rely on dynamic helical systems[15–19] has motivated the development of a variety of chiral actuators where molecules were used either as active transducers of energy[11,13,20,21] or as relays for humidity or temperature changes.[22–25] These soft actuators have demonstrated reversible shape transformation, work, and motility,[26] but the response speed and power produced remain moderate, mainly owing to the lack of mechanisms to drive non-linear actuation.[27] In photosalient crystals, small events are amplified into a large and dramatic mechanical function.[28–31] Herein, we describe a micropatterned liquid-crystal elastomer that accumulates nanoscale deformation, and converts it into rapid movement across length scales. The device mimics seedpod opening by exploiting a fundamental mechanism of stimuli-responsive deformation in plants, namely that flexible and inflexible elements with specific orientations are integrated into the same matrix. Operation is initiated by photochemical isomerization, which drives the opening of two paired polymer strips composing a pod. The handedness of each chiral strip is entirely encoded during microfabrication so that no chiral molecules are required, and the two strips twist in opposite directions until the pod pops open.

Evolution has resulted in plants with slow and continuous molecular-based motion and in strategies for fast and powerful movement as well.[16] For example, in many vetches and in the awns of wild oats and orchids,[32] seed dispersal is triggered by the violent explosion of seedpods, one of the fastest movements in the plant kingdom.[33] Plant pods typically feature a flat hull comprising two narrow sides, with two fibrous layers oriented at angles of $+45°$ and $-45°$ with respect to the longitudinal axis of the pod (Figure 1a). When the pod dries, each fibrous layer shrinks perpendicularly to its orientation, inducing mirror-image saddle-like curvatures and eventually a dramatic opening.[17,18,32] In analogy, we use liquid-crystal networks featuring periodically alternating bars. One set of bars is polymerized in a low liquid-crystalline order state (LO), and the elongation of these bars is consequently negligible under stimulation, whereas the other bars are polymerized while retaining a high liquid-crystalline order (HO); consequently they display anisotropic shape change under illumination (Figure 1b,c).

A liquid crystal was prepared by mixing *trans*-**1** (Figure 1) with liquid-crystal monomers **S1** (see the Supporting Information, Figure S1), a nematic liquid crystal **S2** (Figure S1), and a photoinitiator initiating polymerization with both UV and visible light. A molecular switch was incorporated both to mediate the photopatterning and for encoding the photomechanical behavior of the network after cross-linking. Photoswitch **1** isomerizes under irradiation with UV light ($\lambda = 365$ nm; Figure S2) and relaxes back in the dark ($t_{1/2} \approx 7$ h in hexane). The nematic-to-isotropic transition of the resulting photoresponsive liquid crystal occurs at $T \approx 66\,°C$ (Figure S3).

[*] S. J. Aßhoff, F. Lancia, S. Iamsaard, B. Matt, N. Katsonis
Bio-inspired and Smart Materials
University of Twente
P.O. Box 207, 7500 AE Enschede (The Netherlands)
E-mail: n.h.katsonis@utwente.nl
T. Kudernac
Molecular Nanofabrication Group
University of Twente
P.O. Box 207, 7500 AE Enschede (The Netherlands)
S. P. Fletcher
Department of Chemistry
Chemistry Research Laboratory, University of Oxford
12 Mansfield Road, Oxford OX1 3TA (UK)
E-mail: stephen.fletcher@chem.ox.ac.uk

Supporting information for this article can be found under: http://dx.doi.org/10.1002/anie.201611325.

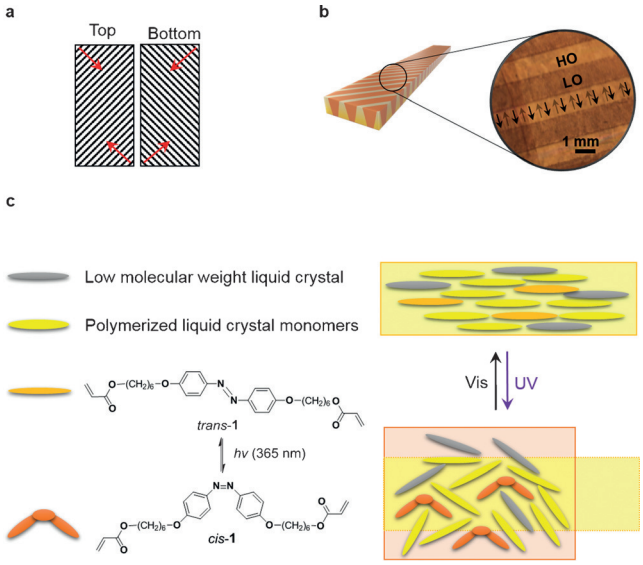

Figure 1. Molecular engineering. a) Rigid fibers are oriented perpendicularly to each other in each of the two valves composing a seedpod. The red arrows indicate the direction in which the material shrinks upon drying. b) Photopatterned liquid-crystal elastomer. c) The photoisomerization of the molecular switch from *trans*-**1** (orange) to *cis*-**1** (red) promotes disorder in the liquid-crystal polymer network and induces anisotropic shape changes in the ordered bars. Polymerized (yellow) and low-molecular-weight (gray) nematic liquid crystals are also found in the liquid-crystal polymer network.

The liquid crystal was introduced into a glass cell where a thin layer of rubbed polyimide was used to align the molecules parallel to the surface. Polymerization was then performed at 60 °C in a two-stage process. The first step involves irradiation with UV light ($\lambda = 365$ nm) through a metal mask (Figure 2a). Irradiation with UV light triggers both photopolymerization and the *trans*-to-*cis* photoisomerization of **1**, providing a lower state of order in the bars that are exposed to UV light. Once UV illumination stops, a large fraction of the azobenzene thermally relaxes back to the *trans* form; however, the polymer network that has been formed in situ keeps the memory of the low degree of order. Next, the cell is flipped upside down, and after removal of the mask, the opposite side of the cell is irradiated with visible light ($\lambda >$ 425 nm) to initiate polymerization in the well-ordered regions (Figure 2a). During the second microfabrication step, polymerization occurs under irradiation with visible light; consequently, photoisomerization of **1** does not occur, and the bars that were covered by the metal mask during the first step polymerize to produce highly ordered bars. The bar patterns are visible under a polarized microscope (Figure 2b and S4) and by visual inspection.

During photopolymerization, the shape of each set of bars will be modified differently because well-aligned liquid-crystal polymer networks shrink anisotropically upon cross-linking, with the largest shrinkage occurring along the orientation direction.[33] Given the orientation of the liquid crystal director in the ordered bars (Figure 1c), their length will change less than their width whereas in the other bars, the extent of the shrinkage is the same in all directions. The final difference in length is distinguishable by optical microscopy (Figure 2b). Once the film is removed from the cell, integration of the bars in the same freestanding material prevents them from reaching their equilibrium length. The polymer film accommodates their different lengths by buckling periodically and bending, a process that has been described in mixed hydrogels.[23,25] Cutting the bar-patterned film leads to a variety of shapes depending on the cutting

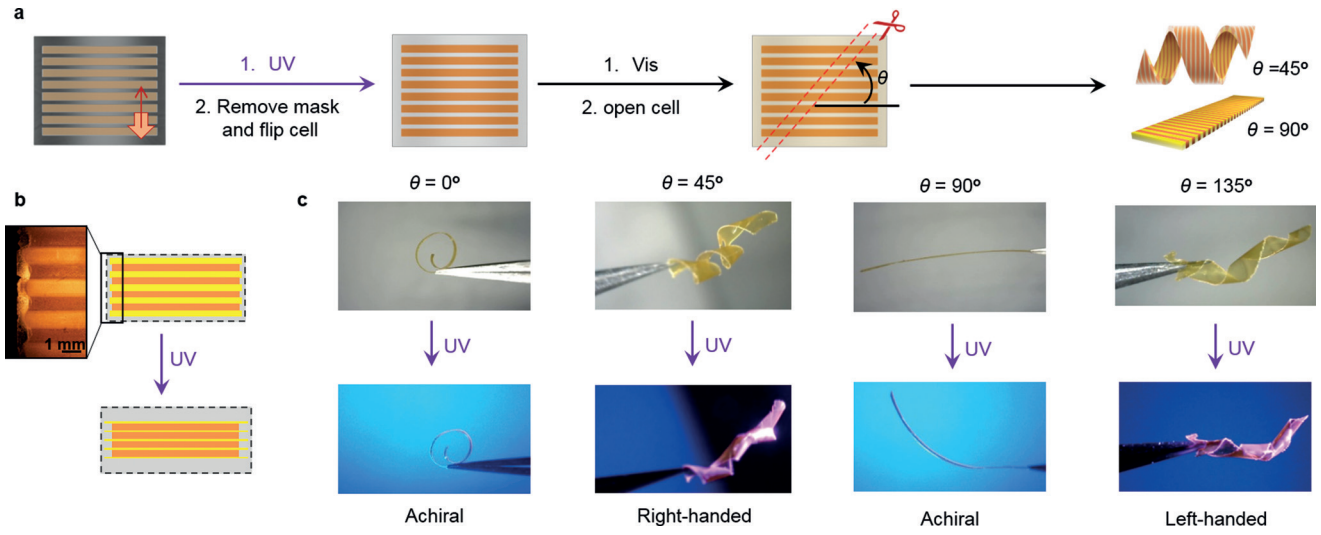

Figure 2. Design and operation of the photopatterned liquid-crystal polymer networks. a) A glass cell is filled with the liquid crystal, heated up to 60 °C, and covered with a mask. After illumination ($\lambda = 365$ nm) for 20 min, the mask is removed, and the cell is flipped upside down. The red arrows represent the rubbing direction of the alignment layer at the top and bottom of the cell. Next the cell is irradiated with visible light ($\lambda >$ 425 nm) for 90 min and subsequently postcured overnight at 60 °C before being opened. The ribbons that are cut out of this film form achiral or chiral shapes depending on the cutting angle. b) An optical microscopy image shows that after cross-polymerization, and in the cell, the highly ordered bars are longer than less ordered ones. Upon illumination, the difference in length is enhanced further. c) Photoinduced shape transitions under illumination. The shape and deformations are reported as a function of the angular offset θ between the axis of the bars and the cutting direction.

angle, that is the offset angle between the long axis of the ribbon and the orientation of the bars (Figure 2a), including flat ribbons and helicoids (Figure 2c).[15] In the absence of any bar pattern, the ribbons do not twist significantly (Figure S5). The chirality of the shapes are determined by the details of the microfabrication process. In the absence of a symmetry-breaking element, the formation of right- and left-handed springs is equally probable, as observed in achiral hydrogels where no difference in structure or composition was implemented across the thickness of the sheet.[23] In the micropatterned material, one specific handedness is associated with a given cutting direction because a density gradient runs across the thickness of the film, which provides a preferred direction for curvature. Gradients in cross-linking density are established during photochemical polymerization because a gradient in light intensity is combined with the diffusion of reactive monomers towards regions that polymerize first.[34] Here, the gradient is established primarily during the first polymerization step, which means that the extent of cross-linking is greater at the top of the cell than at the bottom of the cell. The more densely cross-linked areas will always be found at the outside of the curvature because they are stiffer.[20] Gradients in stiffness have also been reported in twisting plant elements, and the combination of this gradient with a curvature plays a role in determining the handedness of biological helices.[32,33]

We used light to actuate the springs. Under illumination, the *trans*-azobenzene isomerizes and induces an anisotropic deformation of the liquid-crystal network (Figure 1c).[35] This photomechanical property has been used to switch surface roughness[36,37] and to transform twisted shapes before.[13,38,39] In the artificial valves that we designed, the two sets of bars undergo different shape and size modifications upon activation of **1**. In the highly ordered bars, *trans*-to-*cis* isomerization induces expansion preferentially perpendicular to the director, and this specifically translates into an elongation of the bars (Figure 2b). Photochemical isomerization also occurs in the disordered bars but there molecular isomerization is not translated to the macroscopic level efficiently. The shape transformation introduced in the material during polymerization is enhanced further when the polymerized stripes are irradiated with UV light (Figure 3), and the liquid-crystal elastomer compensates for this strain by twisting. This strategy for coupling molecular switches to their functional environment allows for mirror-image springs to twist simultaneously using a single energy source.

We regard the inactive bars as synthetic equivalents of rigid fibers, and the photochemically active highly ordered bars—where azobenzene isomerization is translated into directionally specific polymer deformations—as the equivalent of the soft and deformable matrix in plant tissues. As an indication of the different states of order in the bars, we measured the dichroic ratio of the absorbance of polarized light by the azobenzene in a patterned film, and compared it with two reference films polymerized with UV and visible light. The dichroic ratio was determined before and after activation of the films with UV light. The results (Table S1) confirm that the two types of bars are indeed characterized by different states of order. Comparison to the reference films

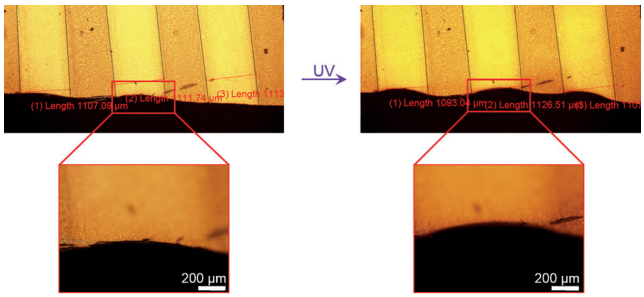

Figure 3. Engineered strain drives the actuation of the device. Upon cross-polymerization, the differential elongation of the patterns in the film generates a side undulation morphology (here shown for $\theta = 90°$, the film was attached to a glass slide with scotch tape at its extremities to prevent curling). Upon illumination, the differential elongation is enhanced further, and so is the lateral undulation morphology; in a free-standing film, this yields a twisting deformation.

also confirmed that the HO bars show a stronger response to UV activation in terms of shape changes.

Next, two mirror-image ribbons were cut, detached from the glass slide, and assembled, that is, each ribbon acted as the valve of an artificial seedpod (Figure 4). Under illumination, the valves initially bend along their long axes; we provisionally attribute the initial bending of the artificial pod to being an artefact of irradiation conditions that are not homogeneous. Next, they bend along their short axes to form a hollow cavity in their center until the valves suddenly detach from each other, twist into springs, and the pod opens. Fast motion thus emerges from a mechanism of amplification where strain builds up slowly and accumulates in a tubular geometry until sudden rupture occurs (Movie S1).

The shape transformation allows for versatility in the action modes. When a weak twist is encoded, more moderate strain builds up so that the pod still opens but only into

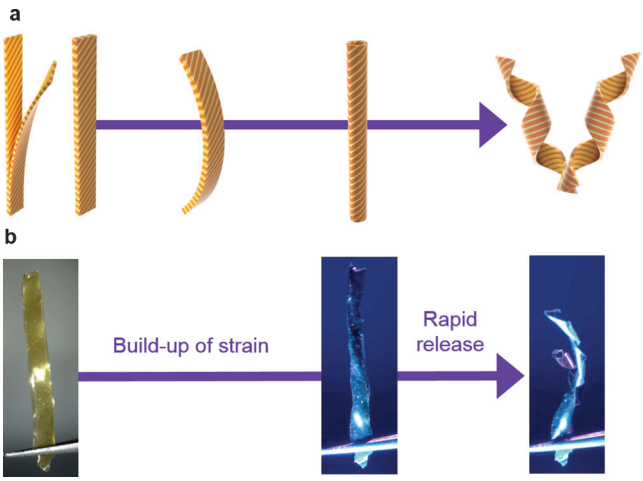

Figure 4. Operation driven by photoinduced strain. The springs are cut at 45° and 135° (width ca. 770 µm, length ca. 1.2 cm), and the total operation process takes about 40 s. a) Stepwise mechanism by which the device pops open. c) The opening is mediated by the formation of a tube (18 s), as also observed in some biological systems. The artificial valves tend to twist in opposite directions, which builds up elastic energy (22 s) until the pod pops open from stress.

a pseudotubular shape. In contrast, for strongly twisting springs, the final valves of the device demonstrate coiling (Figure 5). Varying the angle at which the strips are cut can thus control the amount of strain that accumulates. We note that the opening time (about 40 s for irradiation conditions used for experiments shown in Figure 4) did not vary significantly from one geometry to another.

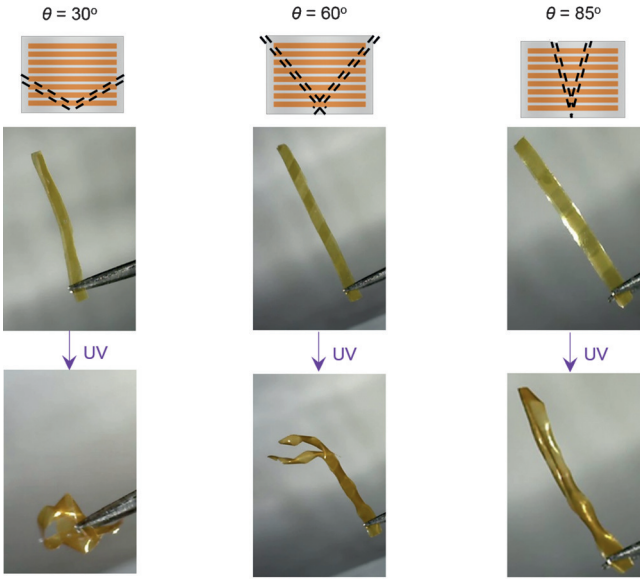

Figure 5. The helical pitch mediates the amount of strain that accumulates. The cutting angle determines the period of the helical ribbons and the maximum strain that can be built up. In devices made of springs that are cut at larger angles ($\theta = 85°$), the final shape remains a tube. At smaller angles ($\theta = 30°$), the final shapes are coiled.

In conclusion, we have developed soft devices where potential energy builds up slowly in the form of elastic energy and is released in a fast event, with potential to produce high-density actuation. The synthetic system consists of two mirror-image valves that are patterned with alternating bars. Each set of bars displays a different shape transformation in response to illumination, leading to a large photomechanical response for each valve and eventually the fast generation of two enantiomeric helices. The chiral materials were prepared solely by fabrication, that is, using only non-chiral molecules. The movement follows strategies seen in plants, where the combination of rigid fibers and deformable soft matter is at the origin of shape transformation. Overall, this work demonstrates that smart materials can be engineered to convert the collective action of molecular switches into a sophisticated and powerful movement resembling evolution-optimized processes of the natural world.

Experimental Section

Materials: The liquid-crystal monomers **S1a**–**S1c** (Synthon chemicals) were mixed in a ratio of **S1a**/**S1b**/**S1c** = 2:3:1 and mixed with 11 wt% of **S2** (Merck). Photoswitch **1** (5.4 wt%; see the Supporting Information for its synthesis) and Irgacure 819 (1 wt%, Ciba) were also added. All compounds were mixed in dichloromethane before the solvent was evaporated to yield the photoresponsive liquid crystal.

Photopatterning of the liquid-crystal elastomer: The liquid crystal was introduced into a 25 μm glass cell with an alignment coating inducing planar alignment of the molecules in antiparallel orientation at the top and bottom surface of the cell. The thin liquid-crystal film was photopolymerized at 60 °C using a pencil lamp for UV light (Spectroline, $\lambda = 365$ nm, 1 mW cm^{-2}) and a halogen lamp equipped with a cut-off filter for visible light ($\lambda > 425$ nm, Edmund Fiber-Lite MI-150 Illuminator, 2.5 mW cm^{-2}). First the cell was irradiated with UV light through a metal mask for 20 min. The width of and distance between the bars were about 950 μm. Subsequently, the mask was removed, and the cell was flipped and irradiated for 90 min with visible light. Then the cell was left in the dark at 60 °C overnight, frozen using liquid nitrogen, and opened with a surgical knife. The strips were cut with a razor blade and manipulated with tweezers.

Light source: The springs and devices were illuminated with a Hönle blue point LED lamp ($\lambda = 365$ nm, 290 mW cm^{-2}).

Acknowledgements

We thank the EPSRC for financial support (Standard Grant EP/M002144/1) and the Royal Society for an International Exchange Grant. N.K. acknowledges financial support from the Dutch Science Foundation (Vidi Grant 700.10.423) and the European Research Council (Starting Grant 307784).

Conflict of interest

The authors declare no conflict of interest.

Keywords: helices · liquid-crystal elastomers · photochromic switches · smart materials

How to cite: *Angew. Chem. Int. Ed.* **2017**, *56*, 3261–3265
Angew. Chem. **2017**, *129*, 3309–3313

[1] T. J. White, D. J. Broer, *Nat. Mater.* **2015**, *14*, 1087.
[2] A. S. Gladman, E. A. Matsumoto, R. G. Nuzzo, L. Mahadevan, J. A. Lewis, *Nat. Mater.* **2016**, *15*, 413.
[3] M. Yamada, M. Kondo, J. Mamiya, Y. Yu, M. Kinoshita, C. J. Barrett, T. Ikeda, *Angew. Chem. Int. Ed.* **2008**, *47*, 4986; *Angew. Chem.* **2008**, *120*, 5064.
[4] B. K. Juluri, A. S. Kumar, Y. Liu, T. Ye, Y.-W. Yang, A. H. Flood, L. Fang, J. F. Stoddart, P. S. Weiss, T. J. Huang, *ACS Nano* **2009**, *3*, 291.
[5] M. Morimoto, M. Irie, *J. Am. Chem. Soc.* **2010**, *132*, 14172.
[6] W. R. Browne, B. L. Feringa, *Nat. Nanotechnol.* **2006**, *1*, 25.
[7] Q. Li, G. Fuks, E. Moulin, M. Maaloum, M. Rawiso, I. Kulic, J. T. Foy, N. Giuseppone, *Nat. Nanotechnol.* **2015**, *10*, 161.
[8] *Molecular switches*, 2nd ed. (Eds.: B. L. Feringa, W. R. Browne), Wiley-VCH, Weinheim, **2011**.
[9] P. Egan, R. Sinko, P. R. LeDuc, S. Keten, *Nat. Commun.* **2015**, *6*, 7418.
[10] J. Deng, J. Li, P. Chen, X. Fang, X. Sun, Y. Jiang, W. Weng, B. Wang, H. Peng, *J. Am. Chem. Soc.* **2016**, *138*, 225.
[11] D. Liu, D. J. Broer, *Angew. Chem. Int. Ed.* **2014**, *53*, 4542; *Angew. Chem.* **2014**, *126*, 4630.
[12] L. T. de Haan, J. M. N. Verjans, D. J. Broer, C. W. M. Bastiaansen, A. P. H. J. Schenning, *J. Am. Chem. Soc.* **2014**, *136*, 10585.
[13] S. Iamsaard, S. J. Aßhoff, B. Matt, T. Kudernac, J. J. M. L. Cornelissen, S. P. Fletcher, N. Katsonis, *Nat. Chem.* **2014**, *6*, 229.

[14] J. C. Nawroth, H. Lee, A. W. Feinberg, C. M. Ripplinger, M. L. McCain, A. Grosberg, J. O. Dabiri, K. K. Parker, *Nat. Biotechnol.* **2012**, *30*, 792.
[15] S. Isnard, A. R. Cobb, N. M. Holbrook, M. Zwieniecki, J. Dumais, *Proc. R. Soc. London Ser. B* **2009**, *276*, 2643.
[16] Y. Forterre, *J. Exp. Bot.* **2013**, *64*, 4745.
[17] Y. Forterre, J. Dumais, *Science* **2011**, *333*, 1715.
[18] R. Elbaum, Y. Abraham, *Plant Sci.* **2014**, *223*, 124.
[19] S. Armon, E. Efrati, R. Kupferman, E. Sharon, *Science* **2011**, *333*, 1726.
[20] S. Iamsaard, E. Villemin, F. Lancia, S. J. Aßhoff, S. P. Fletcher, N. Katsonis, *Nat. Protoc.* **2016**, *11*, 1788.
[21] S. Iamsaard, E. Anger, S. J. Aßhoff, A. Depauw, S. P. Fletcher, N. Katsonis, *Angew. Chem. Int. Ed.* **2016**, *55*, 9908; *Angew. Chem.* **2016**, *128*, 10062.
[22] Y. Sawa, F. Yeb, K. Urayama, T. Takigawa, V. Gimenez-Pinto, R. L. B. Selinger, J. V. Selinger, *Proc. Natl. Acad. Sci. U.S.A.* **2011**, *108*, 6364.
[23] L. Zhang, S. Chizhik, Y. Wen, P. Naumov, *Adv. Funct. Mater.* **2016**, *26*, 1040.
[24] L. Zhang, H. Liang, J. Jacob, P. Naumov, *Nat. Commun.* **2015**, *6*, 7429.
[25] Z. L. Wu, M. Moshe, J. Greener, H. Therien-Aubin, Z. H. Nie, E. Sharon, E. Kumacheva, *Nat. Commun.* **2013**, *4*, 1586.
[26] J. J. Wie, M. R. Shankar, T. J. White, *Nat. Commun.* **2016**, *7*, 13260.
[27] A. Levin, T. C. T. Michaels, L. A. Abramovich, T. O. Mason, T. Müller, B. Zhang, L. Mahadevan, E. Gazit, T. P. J. Knowles, *Nat. Phys.* **2016**, *12*, 926.
[28] P. Commins, I. T. Desta, D. P. Karothu, M. K. Panda, P. Naumov, *Chem. Commun.* **2016**, *52*, 13941.
[29] R. Medishetty, A. Husain, Z. Bai, T. Runcevski, R. E. Dinnebier, P. Naumov, J. J. Vittal, *Angew. Chem. Int. Ed.* **2014**, *53*, 5907; *Angew. Chem.* **2014**, *126*, 6017.
[30] R. Medishetty, S. C. Sahoo, C. E. Mulijanto, P. Naumov, J. J. Vittal, *Chem. Mater.* **2015**, *27*, 1821.
[31] P. Naumov, S. C. Sahoo, B. A. Zakharov, E. V. Boldyreva, *Angew. Chem. Int. Ed.* **2013**, *52*, 9990; *Angew. Chem.* **2013**, *125*, 10174.
[32] D. Koller in *The restless plant* (Ed.: E. Van Volkenburgh), Harvard University Press, Cambridge, **2011**.
[33] H. Hofhuis, D. Moulton, T. Lessinnes, A.-L. Routier-Kierzkowska, R. J. Bomphrey, G. Mosca, H. Reinhardt, P. Sarchet, X. Gan, M. Tsiantis, Y. Ventikos, S. Walker, A. Goriely, R. Smith, A. Hay, *Cell* **2016**, *166*, 222.
[34] D. Liu, D. J. Broer, *Langmuir* **2014**, *30*, 13499.
[35] Y. Yu, M. Nakano, T. Ikeda, *Nature* **2003**, *425*, 145.
[36] D. Liu, D. J. Broer, *Nat. Commun.* **2015**, *6*, 8334.
[37] D. Liu, L. Liu, P. R. Onck, D. J. Broer, *Proc. Natl. Acad. Sci. U.S.A.* **2015**, *112*, 3880.
[38] J. J. Wie, K. M. Lee, T. H. Ware, T. J. White, *Macromolecules* **2015**, *48*, 1087.
[39] K. M. Lee, M. L. Smith, H. Koerner, N. Tabiryan, R. A. Vaia, T. J. Bunning, T. J. White, *Adv. Funct. Mater.* **2011**, *21*, 2913.
[40] R. Elbaum, L. Zaltzman, I. Burgert, P. Fratzl, *Science* **2007**, *316*, 884.

Manuscript received: November 18, 2016
Final Article published: February 9, 2017

